

# Experimental demonstration of tripartite entanglement versus tripartite nonlocality in three-qubit Greenberger-Horne-Zeilinger-class states

Huai-Xin Lu, Jia-Qiang Zhao, Xiao-Qin Wang, and Lian-Zhen Cao

*Department of Physics and Electronic Science, Weifang University, Weifang, Shandong 261061, China*

(Received 22 March 2011; published 20 July 2011)

As stated by S. Ghose *et al.* [*Phys. Rev. Lett.* **102**, 250404 (2009)], there are certain relationships between tripartite entanglement and tripartite nonlocality for three-qubit Greenberger-Horne-Zeilinger (GHZ) class states. In the present work, we have experimentally demonstrated the theoretical results of Ghose *et al.* by using both three-photon generalized GHZ (GGHZ) states and maximal slice (MS) states with a count of  $\sim 10/s$ . From the data, we have verified the agreement of the experimental violation of the Svetlichny inequality with the one predicted by quantum mechanics given the reconstructed density matrix. For the MS states, it is demonstrated that the amount of violation increases linearly following the increase of the degree of tripartite entanglement. In contrast, for GGHZ states, there is a minimal value of the violation when the degree of tripartite entanglement is  $1/3$ . Both of the results are consistent with the theoretical prediction.

DOI: [10.1103/PhysRevA.84.012111](https://doi.org/10.1103/PhysRevA.84.012111)

PACS number(s): 03.65.Ud, 03.67.Bg, 03.67.Mn, 42.65.Lm

## I. INTRODUCTION

Quantum entanglement plays a crucial role in quantum-information processing and the fundamental demonstration of quantum mechanics. Entangled states can be used to demonstrate the contradiction between local reality (LR) and quantum mechanics (QM) [1–4]. It is well known that pure entangled states of two qubits violate the Bell-type Clauser-Horner-Shimony-Holt (CHSH) inequality [5,6], and the amount of violation increases with the degree of the bipartite entanglement [7,8] in the state. The relationship between tripartite entanglement and genuine tripartite nonlocality for three-qubit pure states in the Greenberger-Horne-Zeilinger class has been analyzed by Ghose *et al.* [9]. It is shown that there is unique relationship between tripartite entanglement versus tripartite nonlocality for different types of three-qubit entangled states, such as the generalized Greenberger-Horne-Zeilinger (GGHZ) states and maximal slice (MS) states. The investigation of Bell inequalities for three-qubit states has important meanings for both the practical applications and theoretical studies of quantum entangled states. They are found to have promising applications in the field of quantum communication such as dense coding [10], quantum teleportation [11], and quantum cryptography [12]. In addition, they are useful tools to investigate the entanglement properties of different types of entangled states and prove the genuine multiparty entanglement in the quantum states. Here we focus on the Svetlichny inequality, because its violation is a sufficient condition for the confirmation of genuine three-qubit nonlocal correlations [9].

Experimental demonstration of the Svetlichny inequality with three-qubit GHZ states has been reported [13]. Here, we demonstrate the test of the Svetlichny inequality for the whole set of three-photon GGHZ states and MS states. With the method of quantum-state tomography, we have reconstructed the detailed density matrices of the states and achieved the fidelities of the sources. The average of the fidelity is  $0.84 \pm 0.01$ , comparable to the value in recent work [13], while our intensity is  $\sim 10/s$ . With these sources, we report the experimental testing of the Svetlichny inequality for three-qubit GGHZ states and MS states. Furthermore, we

verify the unique relationship of tripartite entanglement versus tripartite nonlocality for each type of these quantum states, as predicted in Ref. [9].

## II. THEORY

Svetlichny considered a hybrid model of nonlocal-local realism where two of the qubits are nonlocally correlated, but are locally correlated to the third. The Svetlichny inequality is defined in terms of the expectation value of a Bell-type operator  $S$ , which is defined as

$$S = A(BK + B'K') + A'(BK' - B'K), \quad (1)$$

where  $K = C + C'$  and  $K' = C - C'$ . There are three spatially separated qubits, and the operator  $A = \vec{a} \cdot \vec{\sigma}_1$  or  $A' = \vec{a}' \cdot \vec{\sigma}_1$  is performed on qubit 1,  $B = \vec{b} \cdot \vec{\sigma}_2$  or  $B' = \vec{b}' \cdot \vec{\sigma}_2$  on qubit 2, and  $C = \vec{c} \cdot \vec{\sigma}_3$  or  $C' = \vec{c}' \cdot \vec{\sigma}_3$  on qubit 3, where  $\vec{a}$ ,  $\vec{a}'$ ,  $\vec{b}$ ,  $\vec{b}'$ , and  $\vec{c}$ ,  $\vec{c}'$  are unit vectors,  $\vec{\sigma}_i$  are spin projection operators, and  $\vec{a}' = (\sin \theta_a \cos \phi_a, \sin \theta_a \sin \phi_a, \cos \theta_a)$ . If a theory is consistent with a hybrid model of nonlocal-local realism, the expectation value for any three-qubit state is bounded by the Svetlichny inequality,  $|\langle \psi | S | \psi \rangle| = S(\psi) \leq 4$ .

The GGHZ state  $|\psi_g\rangle$  and the MS states  $|\psi_s\rangle$  are defined as follows [9]:

$$|\psi_g\rangle = \cos \theta_1 |000\rangle + \sin \theta_1 |111\rangle, \quad (2)$$

$$|\psi_s\rangle = \frac{1}{\sqrt{2}} \{ |000\rangle + |11\rangle (\cos \theta_3 |0\rangle + \sin \theta_3 |1\rangle) \}. \quad (3)$$

The maximum expectation values of  $S$  for the GGHZ and MS states are respectively

$$S_{\max}(\psi_g) = \begin{cases} 4\sqrt{1 - \tau(\psi_g)}, & \tau(\psi_g) \leq 1/3, \\ 4\sqrt{2\tau(\psi_g)}, & \tau(\psi_g) \geq 1/3, \end{cases} \quad (4)$$

$$S_{\max}(\psi_s) = 4\sqrt{1 + \tau(\psi_s)}, \quad (5)$$

where the three-tangle  $\tau(\psi)$  quantifies tripartite entanglement [14], with  $\tau(\psi_g) = \sin^2 2\theta_1$  and  $\tau(\psi_s) = \sin^2 \theta_3$ . Ghose *et al.* show theoretically that, for MS states, the amount of violation increases linearly following the increase of the degree of

TABLE I. Special angles chosen in our experiment. Several special angles  $\theta_3 = 90^\circ, 58^\circ, 40^\circ$ , and  $22^\circ$ , can be derived from the experiment data. From  $\theta_3$ , we can calculate  $\theta_c = \theta_{c'} = \arctan(\sqrt{2} \tan \theta_3) = 90^\circ, 66.2^\circ, 49.9^\circ$ , and  $29.7^\circ$ , respectively.

	$\theta_a$	$\theta_{a'}$	$\theta_c$	$\theta_{c'}$	$\theta_d$	$\theta_{d'}$
$\tau(\psi_g) \leq 1/3$	0	0	0	0	$\pi$	0
$\tau(\psi_g) \geq 1/3$	$\pi/2$	$\pi/2$	$\pi/2$	$\pi/2$	$\pi/2$	$\pi/2$
MS states	$\pi/2$	$\pi/2$	$\arctan(\sqrt{2} \tan \theta_3)$	$\arctan(\sqrt{2} \tan \theta_3)$	$\pi/2$	$\pi/2$
	$\phi_a$	$\phi_{a'}$	$\phi_c$	$\phi_{c'}$	$\phi_d$	$\phi_{d'}$
$\tau(\psi_g) \leq 1/3$	/	/	/	/	/	/
$\tau(\psi_g) \geq 1/3$	$-\pi/2$	0	0	$\pi/2$	$\pi/2$	0
MS states	$\pi/4$	$-\pi/4$	$\pi/4$	$-\pi/4$	$\pi/2$	0

tripartite entanglement, while for GGHZ states,  $S_{\max}(\psi_g)$  initially decreases monotonically with  $\tau$ , and then increases for  $\tau(\psi_g) > 1/3$ .

According to Ref. [9], to achieve  $S_{\max}(\psi_g)$  in Eq. (4), we could measure by the following possible sets of unit vectors: for  $\tau(\psi_g) \leq 1/3$ ,  $\vec{a}, \vec{a}', \vec{b}, \vec{b}'$ , and  $\vec{c}$  are all aligned along  $\vec{z}$ , and  $\vec{c}'$  is aligned along  $-\vec{z}$ ; for  $\tau(\psi_g) \geq 1/3$  all the measurement vectors lie in the  $x$ - $y$  plane with  $\phi_{adc} = \phi_{ad'c'} = \phi_{a'd'c} = 0$ ,  $\phi_{a'dc'} = \pi$ , and  $\phi_d - \phi_{d'} = \pi/2$ , where  $\phi_{ijk}$  is defined as  $\phi_{ijk} = \phi_i + \phi_j + \phi_k$ . The theoretical values of the lower and upper bounds are consistent with the numerical bounds in Ref. [15].

With respect to the MS state, a set of measurement angles which realize  $S_{\max}(\psi_s)$  in Eq. (5) is  $\theta_a = \theta_{a'} = \theta_d = \theta_{d'} = \pi/2$ ,  $\tan \theta_c = \tan \theta_{c'} = \sqrt{2} \tan \theta_3$ ,  $\phi_{adc} = \phi_{ad'c'} = \phi_{a'd'c} = 0$ ,  $\phi_{a'dc'} = \pi$ ,  $\phi_c = -\phi_{c'} = \pi/4$ , and  $\phi_d - \phi_{d'} = \pi/2$ . The only difference between these angles and the optimal measurement angles for the GGHZ states in the regime  $\tau(\psi_g) > 1/3$  is that  $\vec{c}$  and  $\vec{c}'$  do not lie in the  $x$ - $y$  plane. In our experiment, we choose a set of special angles as Table I.

### III. EXPERIMENTAL SETUP

The first step of the experiment is to generate polarization-entangled three-qubit GHZ states. Following our previous work [16], as shown in Fig. 1, a mode-locked Ti:sapphire laser outputs an infrared (IR) pulse with a central wavelength of 780 nm, a pulse duration of 100 fs, and a repetition of 80 MHz, which passes through a LiB<sub>3</sub>O<sub>5</sub> (LBO) crystal and is converted to an ultraviolet (uv) light pulse with a central wavelength of 390 nm. Then the uv light pulse passes through five dichroic mirrors (DMs) which are used to separate the mixed infrared and ultraviolet light components. Behind the five DMs, the uv light is focused on a  $\beta$ -barium borate (BBO) crystal to produce a pair of entangled photons ( $|H_2H_3\rangle + |V_2V_3\rangle$ )/ $\sqrt{2}$  in paths 2 and 3, while the transmitted ir light is attenuated to a weak pseudo-single-photon source which is prepared in the state ( $|H_1\rangle + |V_1\rangle$ )/ $\sqrt{2}$  in path 1, where  $H$  and  $V$  represent horizontal and vertical polarization separately. Then, photon 2 is combined with photon 1 on a polarizing beam splitter (PBS<sub>12</sub>). By finely adjusting the delay between paths 1 and 2 to make sure photon 1 and photon 2 arrive at the PBS<sub>12</sub> simultaneously, the three-qubit GHZ states  $|\psi_{\text{GHZ}}\rangle = \frac{1}{\sqrt{2}}(|HHH\rangle + |VVV\rangle)$  can be obtained. In order to get a better fidelity of the output states, we lowered the average power of

the laser to 90 mW, and the two-photon coincidence count rate to  $6 \times 10^3 \text{ s}^{-1}$ . The visibility of the two-photon entangled state is 97% in the  $H$  ( $V$ ) basis and 95% in the  $+$  ( $-$ ) basis, where  $|+\rangle = \frac{1}{\sqrt{2}}(|H\rangle + |V\rangle)$ ,  $|-\rangle = \frac{1}{\sqrt{2}}(|H\rangle - |V\rangle)$ . We use the maximum-likelihood technique to construct the density matrix of the state, and from the estimated density matrix, we calculate the fidelity characterizing the quality of the state as  $F = \langle \psi_{\text{GHZ}} | \rho | \psi_{\text{GHZ}} \rangle = 0.84 \pm 0.01$ .

Next, we generate the GGHZ states and MS states based on the setup from which we get the GHZ states. In order to obtain the GGHZ state  $|\psi_g\rangle$ , we used a half-wave plate (HWP<sub>1</sub>) (see Fig. 1), which is placed behind PBS<sub>1</sub> and set at an angle  $\theta_1$ . The photon 1 after HWP<sub>1</sub> is prepared in the state  $(\cos \theta_1 |H\rangle + \sin \theta_1 |V\rangle)/\sqrt{2}$ . By superposing photon 1 with photon 2 on PBS<sub>2</sub>, we can get a three-qubit state:

$$|\psi\rangle_{\text{GGHZ}} = \cos \theta_1 |V_1 V_2 V_3\rangle + \sin \theta_1 |H_1 H_2 H_3\rangle. \quad (6)$$

For instance, by choosing  $\theta_1 = \pi/4$ , the output states will be  $\frac{1}{\sqrt{2}}(|HHH\rangle + |VVV\rangle)$ , which is exactly GHZ states. From the experimental results, we calculate  $\theta_1$  by following the equality

$$\theta_1 = \arcsin \sqrt{N_{HHH}/(N_{HHH} + N_{VVV})}, \quad (7)$$

where  $N_{HHH}$  and  $N_{VVV}$  denote three-fold coincidence counts in the basis  $H_1 H_2 H_3$  and  $V_1 V_2 V_3$ . In the experiment, we have measured the fidelity and Svetlichny inequality at nine points, which have the proportion of  $N_{HHH}/N_{VVV}$  as 1:1, 1:2, 1:4, 1:6, 1:8, 1:10, 1:14, 1:20, and 1:60. This will correspond to  $\theta_1 = 45^\circ, 35.3^\circ, 26.6^\circ, 22.2^\circ, 19.5^\circ, 17.5^\circ, 15^\circ, 12.6^\circ$ , and  $7.4^\circ$ , respectively.

Compared to the generation of the GGHZ states, it is more complicated to generate the MS state  $|\psi_s\rangle$ . We carry out the following steps to produce this state. First, HWP<sub>1</sub> is set at  $\pi/8$ , which will result a three-qubit GHZ state  $\frac{1}{\sqrt{2}}(|H_1 H_2 H_3\rangle + |V_1 V_2 V_3\rangle)$ . Second, we insert another half-wave plate HWP<sub>3</sub> in path 3, which is set at  $22.5^\circ$  and can make the change  $|H_3\rangle \rightarrow |+_3\rangle$ ,  $|V_3\rangle \rightarrow |-_3\rangle$ . This will convert the GHZ state into  $\frac{1}{\sqrt{2}}(|H_1 H_2 +_3\rangle + |V_1 V_2 -_3\rangle)$ . Then, we use a polarization dependent beam splitter cube (PBC), which has properties as follows: It transmits the horizontal polarization photons with the probability  $a^2$ , while for the vertical polarization, the transmission is  $b^2$ . The PBC is a custom-made component. The values of  $a$  and  $b$  can be adjusted through the changing of the axis of PBC. After the PBC, the

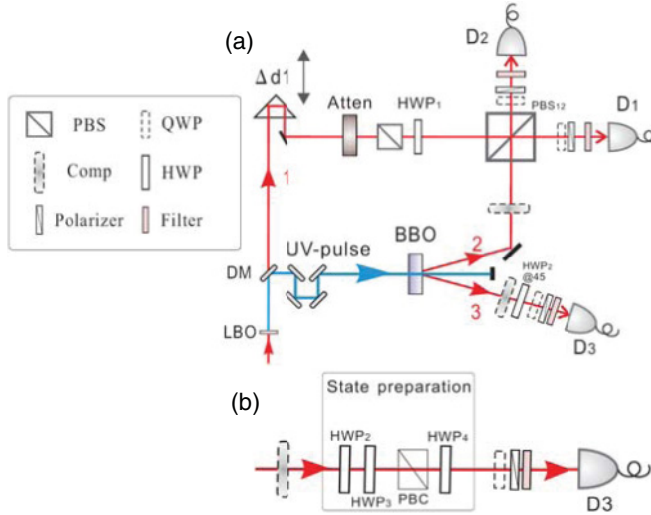


FIG. 1. (Color online) Scheme of the experimental setup. (a) The setup to generate the required three-photon GHZ state, here setting HWP<sub>2</sub> at 45°. The entangled photons are generated by pumping the uv laser beam on a BBO crystal and a pseudo-single-photon source is prepared by attenuating the infrared light after the DM. The average power in the experiment is 90 mW and the average twofold coincidence is  $6 \times 10^3 \text{ s}^{-1}$  in modes 2 and 3. Prism  $\Delta d_1$  is used to ensure that the input photons arrive at the PBS<sub>12</sub> at the same time. Half-wave plate (HWP) 1 is used to prepare the single-photon state  $\frac{1}{\sqrt{2}}(|H\rangle_1 + |V\rangle_1)$  and HWP<sub>2</sub> is used to prepare the desired two-photon state. To achieve good temporal and spatial overlap at PBS<sub>12</sub>, every output is spectrally filtered ( $\Delta F_{\text{WHM}} = 3 \text{ nm}$ ) and monitored by fibre coupled single-photon detectors. Throughout the experiment, the coincidence time window is set to be 5 ns, which ensures that accidental coincidence is negligible. (b) Setup for preparing the MS state. HWP<sub>1</sub> is set at  $\pi/8$ , and the superposed three-qubit state is GHZ state  $\frac{1}{\sqrt{2}}(|H_1 H_2 H_3\rangle + |V_1 V_2 V_3\rangle)$ . Then we set HWP<sub>3</sub> at 22.5° and can make the change  $|H_3\rangle \rightarrow |+_3\rangle$ ,  $|V_3\rangle \rightarrow |-_3\rangle$ . This will convert the GHZ state into  $\frac{1}{\sqrt{2}}(|H_1 H_2 +_3\rangle + |V_1 V_2 -_3\rangle)$ . After that we use a polarization dependent beam splitter cube (PBC). Therefore the state is  $\frac{1}{\sqrt{2}}[|H_1 H_2\rangle(a|H_3\rangle + b|V_3\rangle) + |V_1 V_2\rangle(a|H_3\rangle - b|V_3\rangle)]$ , then another half-wave plate (HWP<sub>4</sub>) setting at an angle chosen according to the transmissions  $a$  and  $b$  is used behind PBC. Its function is as follows: It changes  $a|H_3\rangle + b|V_3\rangle \rightarrow |H_3\rangle$ , while  $a|H_3\rangle - b|V_3\rangle \rightarrow \cos \theta_3 |H_3\rangle + \sin \theta_3 |V_3\rangle$ .

state becomes  $\frac{1}{\sqrt{2}}[|H_1 H_2\rangle(a|H_3\rangle + b|V_3\rangle) + |V_1 V_2\rangle(a|H_3\rangle - b|V_3\rangle)]$ . Finally, another half-wave plate (HWP<sub>4</sub>) is placed behind the PBC and is set at a chosen angle according to the transmissions  $a$  and  $b$ . It has the function as follows:  $a|H_3\rangle + b|V_3\rangle \rightarrow |H_3\rangle$ , and  $a|H_3\rangle - b|V_3\rangle \rightarrow \cos \theta_3 |H_3\rangle + \sin \theta_3 |V_3\rangle$ , where  $\theta_3 = \arcsin [b/(a + b)]^{1/2}$ . All these steps will result a MS state as

$$|\psi_s\rangle = \frac{1}{\sqrt{2}}\{|H_1 H_2 H_3\rangle + |V_1 V_2\rangle(\cos \theta_3 |H_3\rangle + \sin \theta_3 |V_3\rangle)\}. \quad (8)$$

#### IV. EXPERIMENTAL RESULT

In order to characterize the prepared three-qubit GHZ states and MS states for different  $\theta_1$  and  $\theta_3$ , we have extracted their density matrices by the method of overcomplete-state

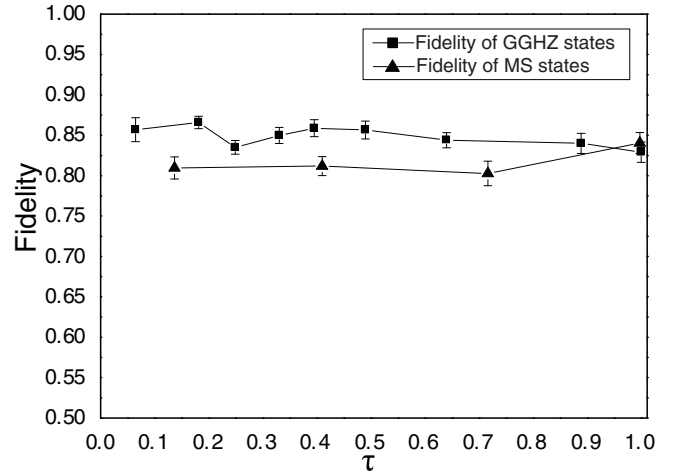


FIG. 2. Fidelity of GHZ states and MS states. The fidelity equals  $\langle \psi | \rho | \psi \rangle$ . Each experimental value is obtained by measuring in an average time of 120 seconds. The error bar of the fidelity is calculated by performing a 100 run Monte Carlo simulation of the whole state tomography analysis, with Poissonian noise added to each experimental datum in each run.

tomography [17]. This is implemented by collecting the experimental data for 20 s for each of 216 combinations of measurement basis  $\{|H\rangle, |V\rangle, |+\rangle, |-\rangle, |R\rangle, |L\rangle\}$ , where  $|R\rangle = \frac{1}{\sqrt{2}}(|H\rangle + i|V\rangle)$  and  $|L\rangle = \frac{1}{\sqrt{2}}(|H\rangle - i|V\rangle)$ . With these data, the maximum-likelihood technique is used to construct the density matrix of the state. The results are shown in Fig. 2, from which we can see that the fidelities of GHZ states and MS states for different  $\theta_1$  and  $\theta_3$  are all larger than 0.8.

Based on the generated state in Eqs. (8) and (10) and the special chosen angles in Eqs. (6) and (7), we have measured the Svetlichny inequality. The concrete results are given in Fig. 3. For each measurement point, we have collected the data for

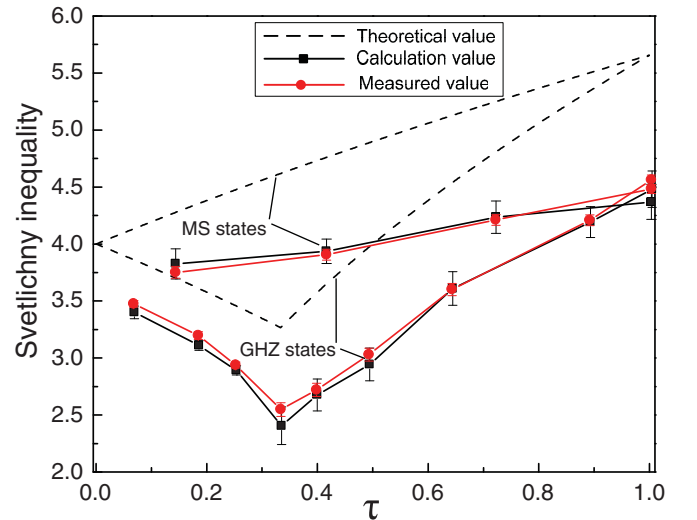


FIG. 3. (Color online) Experimental results. The dashed line shows the plot of Eqs. (3) and (4) for  $S_{\text{max}}(\psi_g)$  versus  $\tau$  for the GHZ states [9]. The labeled lines show the experimental result of Svetlichny inequalities, where the calculation value is calculated from the state density matrix and the measured value is the measured value of the Svetlichny operator.

120 s. In Fig. 3, we have plotted the experimental Svetlichny operator values and the one calculated from the estimated state density matrices. The theoretical values are also drawn using a dashed line in Fig. 3. From the experimental results, we can draw three conclusions: First, the experimental violation of the Svetlichny inequality is quite consistent with the one predicted by quantum mechanics given the reconstructed density matrix; second, for the MS states, the amount of violation increases linearly following the increase of the degree of tripartite entanglement, while for GHZ states there is a minimal value of the violation when the degree of tripartite entanglement is  $1/3$ . Third, the experimental values of the violation are smaller than the theoretical values. There are two important reasons for the experimental nonideal data. On the one hand, the multipair generation of entangled states contributes the main noise of the results due to the probabilistic character of the parametric down-conversion sources. On the other hand, the imperfection of the linear optics elements such as the beam splitter also makes the results nonideal.

## V. CONCLUSION

In summary, in our experiment, series of GHZ states and MS states with high fidelity  $F > 0.8$  have been prepared and we have demonstrated the test of the Svetlichny inequality with these states. Tripartite entanglement versus tripartite nonlocality in three-qubit GHZ-class states has been experimentally reported.

There are many open experimental and theoretical questions which are worthy of investigation in the future. Theoretically, it is interesting to generalize the relationship of entanglement and nonlocality to the case of entangled states with more than three qubits. Also, it is worth studying the Svetlichny inequality for other types of state, such as the  $W$  state [18]. Third, since there is a certain relationship of multipartite entanglement and nonlocality, we could use certain Bell inequalities to detect genuine multiparty entanglement. For a specific state, how to obtain the optimum witness is an important research direction. Finally, there are various types of Bell inequalities for three-qubit generalized GHZ states, such as the MABK (Mermin-Ardehali-Belinskii-Klyshko) inequality [19–21], the Gisin inequality [22], the Zukowski-Brukner inequality [23,24], and the Svetlichny inequality [25]. In the future, it would be interesting to investigate which one is more robust against the noise, and thus more suitable to characterize states.

## ACKNOWLEDGMENTS

We thank Wei-Bo Gao for valuable discussions. This work was supported by the Natural Science Foundation of China (Grant No. 60878001), the Natural Science Foundation of Shandong Province (Grant No. Y2006A24), and the Science and Technology Development Program of Shandong Province (Grant No. 2010GGX10118).

- 
- [1] W. Tittel, J. Brendel, H. Zbinden, and N. Gisin, *Phys. Rev. Lett.* **81**, 3563 (1998).
  - [2] N. Gisin, *Science* **326**, 1357 (2009).
  - [3] D. N. Matsukevich, P. Maunz, D. L. Moehring, S. Olmschenk, and C. Monroe, *Phys. Rev. Lett.* **100**, 150404 (2008).
  - [4] J. L. Chen and D. L. Deng, *Phys. Rev. A* **79**, 012115 (2009).
  - [5] P. R. Tapster, J. G. Rarity, and P. C. M. Owens, *Phys. Rev. Lett.* **73**, 1923 (1994).
  - [6] J. F. Clauser, M. A. Horne, A. Shimony, and R. A. Holt, *Phys. Rev. Lett.* **23**, 880 (1969).
  - [7] N. Gisin, *Phys. Lett. A* **154**, 201 (1991).
  - [8] S. Popescu and D. Rohrlich, *Phys. Lett. A* **166**, 293 (1992).
  - [9] S. Ghose, N. Sinclair, S. Debnath, P. Rungta, and R. Stock, *Phys. Rev. Lett.* **102**, 250404 (2009).
  - [10] H. A. Carteret and A. Sudbery, *J. Phys. A* **33**, 4981 (2000).
  - [11] J. C. Howell, A. Lamas-Linares, and D. Bouwmeester, *Phys. Rev. Lett.* **88**, 030401 (2002).
  - [12] K. Mattle, H. Weinfurter, P. G. Kwiat, and A. Zeilinger, *Phys. Rev. Lett.* **76**, 4656 (1996).
  - [13] J. Lavoie, R. Kaltenbaek, and K. J. Resch, *New J. Phys.* **11**, 073051 (2009).
  - [14] V. Coffman, J. Kundu, and W. K. Wootters, *Phys. Rev. A* **61**, 052306 (2000).
  - [15] C. Emary and C. W. J. Beenakker, *Phys. Rev. A* **69**, 032317 (2004).
  - [16] H. X. Lu, J. Zhang, X. Q. Wang, Y. D. Li, and C. Y. Wang, *Phys. Rev. A* **78**, 033819 (2008).
  - [17] K. J. Resch, P. Walther, and A. Zeilinger, *Phys. Rev. Lett.* **94**, 070402 (2005).
  - [18] W. Dur, G. Vidal, and J. I. Cirac, *Phys. Rev. A* **62**, 062314 (2000).
  - [19] N. D. Mermin, *Phys. Rev. Lett.* **65**, 1838 (1990).
  - [20] M. Ardehali, *Phys. Rev. A* **46**, 5375 (1992).
  - [21] A. V. Belinskii and D. N. Klyshko, *Phys. Usp.* **36**, 653 (1993).
  - [22] J. L. Chen, C. Wu, L. C. Kwek, and C. H. Oh, *Phys. Rev. A* **78**, 032107 (2008).
  - [23] M. Zukowski, C. Brukner, W. Laskowski, and M. Wiesniak, *Phys. Rev. Lett.* **88**, 210402 (2002).
  - [24] M. Zukowski and C. Brukner, *Phys. Rev. Lett.* **88**, 210401 (2002).
  - [25] G. Svetlichny, *Phys. Rev. D* **35**, 3066 (1987).